ROTORDYNAMICS ON THE MINICOMPUTER*

by

Edgar J. Gunter, Professor
Department of Mechanical and Aerospace Engineering
Director, Rotor Dynamics Laboratory
University of Virginia
Charlottesville, Virginia 22901

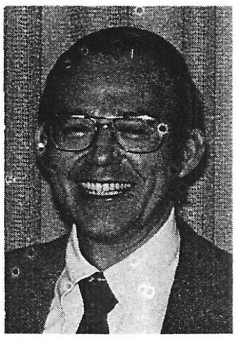

Edgar J. Gunter, Jr., has been the principal investigator of the dynamic characteristics of rigid and flexible rotors for NASA Lewis Research Center since 1966. Other research projects have had to do with nonlinear analysis of squeeze-film dampers, stabilization of turbomachinery, and the dynamic analysis of the space shuttle main engine -- high pressure fuel turbopump. Gunter is also Director of an industrial supported program on dynamic analysis of turbomachinery. He holds a Ph.D. in Engineering Mechanics from the University of Pennsylvania and is a member of ASME and Tau Beta Pi.

INTRODUCTION

This paper deals with the investigation, using a minicomputer, of the theoretical and experimental behavior of a multimass test rotor mounted in fluid film journal bearings. The minicomputer has been used to analyze the rotor critical speeds, bearing coefficients, unbalance response, and stability characteristics. The minicomputer was also employed to sample, collect and reduce the experimental rotor characteristics to obtain the rotor amplification factor at the first critical speed.

The use of a minicomputer system to both analyze the theoretical rotor behavior and to evaluate the experimental rotor motion has added a new dimension to the state of the art in machinery analysis.

CRITICAL SPEED ANALYSIS OF CENTRITECH ROTOR

The Rotor Dynamics Laboratory of the University of Virginia has over the past several years tested various flexible rotors in fluid film journal bearings to evaluate the rotor characteristics of stability and unbalance response. The experimental test facility was developed and built for the Rotor Dynamics Laboratory by the Centritech Corporation. Several rotors, with various numbers of discs and shaft diameters have been built and tested. One configuration in particular that has received a considerable amount of attention in the past two years is the design referred to as the "3-mass model". This rotor was designed to simulate a class of high-speed multistage compressors that operate up to speeds of 12,000 RPM and have a first critical speed around 3,000 RPM, and a second critical speed near 10,000 RPM. This class of compressor has in the past proven to be very susceptible to self-excited whirl instability caused by either the bearings, seals, or aerodynamic cross coupling forces acting at the compressor stations.

Figure 1 represents a schematic cross section of the 3-mass Centritech test rotor. The rotor weighs 29 lbs, is 26 inches long and has a bearing span of 21 inches. The rotor facility also has movable proximity probe holders to monitor the rotor motion. Figure 1 represents the cross section of the 3-mass Centritech rotor as modeled on the HP-9845 computer. A total of 21 mass stations were used in the analysis. A brief summary of the matrix transfer equations and the input to the computer program is given in Appendix A. Numerical difficulties are often experienced with the matrix transfer process. Because of round-off errors, the number of stations that can be used in a program is limited to around 40 stations. The limitations encountered with the matrix transfer method are also dependent upon the type of computer used and the number of significant figures that can be carried. The need for double precision arithmetic for the matrix transfer calculations arises from the condition that the off diagonal elements may become of order ε in comparison to the main diagonal elements. The successive multiplication of matrixes with off diagonal terms several orders of magnitude below the main diagonal terms rapidly leads to numerical instability. The matrix transfer algorithm employed in the desk top HP-9845 computer program has been normalized in order to improve the computational accuracy. The new procedure developed and used in this program greatly alleviates some of the numerical difficulties encountered with the matrix transfer method. For example, a 70 station turbine has been successfully analyzed using this program.

Table 1 represents the rotor cross

*Report No. UVA/643078/MAE80/105
November 1980

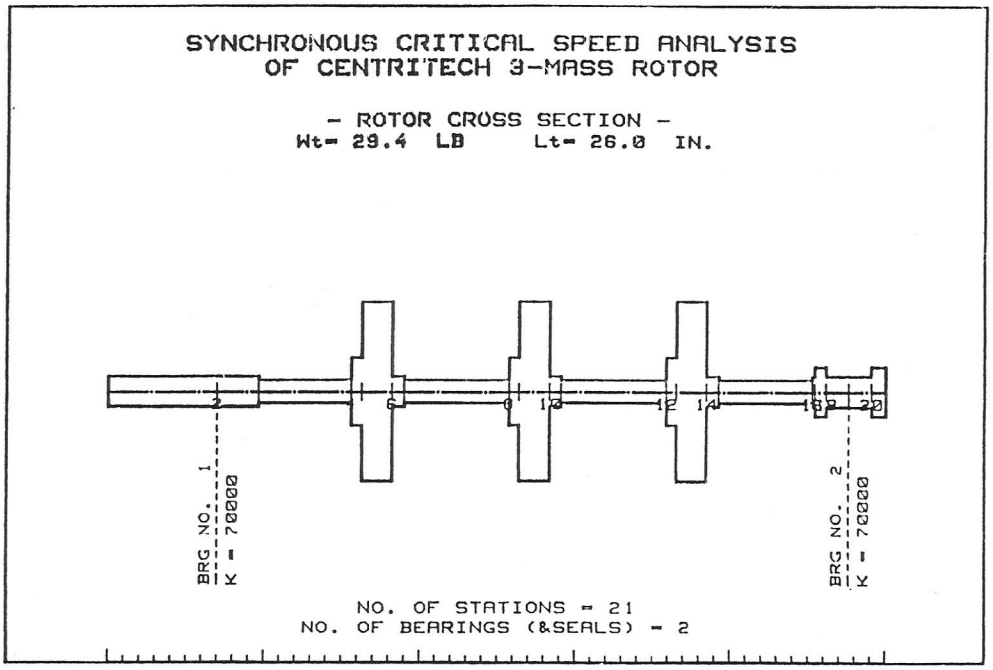

Figure 1. Cross Section of Centritech 3-Mass Rotor

sectional properties. The rotor cross section is read into the program (see Appendix A) and the station weights and inertia properties are automatically calculated by the computer program. As can be seen from the tabular summary, the total rotor weight is 29.4 lbs. and the length is 26 in. The computer program also calculates the center of gravity of the rotor which is 14.0 inches from the left end. Hence, the rotor is not exactly symmetric and the rotor mode shapes will not be perfectly symmetric (or asymmetric about the rotor midpoint).

Table 2 represents the undamped critical speed mode shapes and strain energy distribution, including transverse shear deformation for the Centritech 3-mass rotor for the first two critical speeds. The first column represents the dimensionless shaft displacement. The mode shape is normalized to unity. The second column represents the slope of the mode shape. The third and fourth columns represent the moment and shear distribution along the shaft. The first critical speed for the bearing spring rate of 70,000 lb/in was found to be 2,580 RPM. The matrix transfer procedure required five iterations to converge to the proper solutions. In the particular case run, the ends of the rotor were assumed to be free-free. This implies that the shear and moment acting at the ends of the rotor are zero. As a check on the accuracy on the computer program, it can be seen that the shear and moment listed in the tables are zero. Table 2 also represents the relative strain energy distributed in the shaft and the bearings. Note that in the first critical speed, only 2 percent of the total strain energy is in the bearings. For the first mode, 39 percent of the strain energy is distributed between substations 7 and 8 and 38 percent is distributed between stations 11 to 12. These are the two lengths on either side of the center impeller. Therefore, it is readily apparent that if one wishes to increase the resonance frequency of the first mode, then the most expedient section of the shaft to stiffen would be these two spans. Note that little increase in the first critical speed of this rotor could be achieved by increasing the bearing stiffness.

Table 3 represents a critical speed summary for the 3-mass rotor for the first three synchronous critical speeds. The synchronous critical speeds listed in the table are 2,580 RPM, 10,692 RPM and 26,389 RPM for the third mode. The modal weight corresponding to each mode is given along with the modal inertia. If the modal inertia is small in comparison to the modal weight, then gyroscopic effects will have little influence on shifting this particular critical speed. The modal weight and modal inertia components are given by the following equations:

$$M_i = \int_0^L P\phi_i^2 \, dx = \sum_{j=1}^{N} W_j \phi_{ij}^2$$

$$I_{ti} = \int_0^L I_t(x) \phi'^2 \, dx = \sum_{j=1}^{N} I_{tj} \phi_{ij}'^2$$

Table 1. Sectional Properties of 3-Mass Centritech Rotor

SYNCHRONOUS CRITICAL SPEED ANALYSIS
OF CENTRITECH 3-MASS ROTOR

N= 21 NBRG= 2 NCASE= 1 NMODES= 3 Eps= .001000

ROTOR WEIGHT= 29.41 , LENGTH= 25.99 , C.G.= 14.07 FROM LEFT

I	W(LBS)	L(I)	D(I)	EI	IP	IT
1	.40	3.64	1.00	1.448E+06	.1	.5
2	.56	1.38	1.00	1.448E+06	.1	.5
3	.35	3.10	.75	4.582E+05	.0	.2
4	.39	.35	2.25	3.718E+07	.1	.2
5	4.22	1.00	6.01	1.885E+09	18.3	9.5
6	4.07	.40	1.00	1.448E+06	18.2	9.4
7	.26	3.52	.75	4.582E+05	.0	.2
8	.40	.33	2.25	3.724E+07	.1	.3
9	4.32	1.03	6.01	1.885E+09	18.7	9.7
10	4.17	.39	1.00	1.448E+06	18.6	9.7
11	.26	3.51	.75	4.582E+05	.0	.2
12	.41	.33	2.25	3.731E+07	.1	.3
13	4.21	1.00	6.01	1.885E+09	18.3	9.5
14	4.07	.41	1.00	1.448E+06	18.2	9.4
15	.24	3.12	.75	4.582E+05	.0	.2
16	.20	.09	1.00	1.448E+06	.0	.2
17	.12	.38	1.63	1.010E+07	.0	.0
18	.19	.76	1.00	1.448E+06	.0	.0
19	.17	.76	1.00	1.448E+06	.0	.0
20	.23	.50	1.63	1.010E+07	.1	.0
21	.15	0.00	1.00	1.448E+06	.0	.0
	29.4	26.0	1.91	2.763E+08		

BEARING STATION LOCATIONS
BRG. NO. 1 = 2 BRG. NO. 2 = 19

BRG. STIFFNESS VALUES

BRG. NO. 1 ST. 2 K= 70000 LB/IN
BRG. NO. 2 ST. 19 K= 70000 LB/IN

ROTOR BOUNDARY CONDITIONS ARE FREE-FREE
WHIRL MOTION IS S
Irpm= 2000 Drpm= 500 Frpm= 30000

L1AVG= 1.721E-06 L2AVG= 2.694E-06 L3AVG= 2.971E-06

In addition to the modal weight, the modal Table 3B represents the critical speeds assuming planar modes, and the corresponding planar modes are computed. These planar modes may be used as a set of orthogonal functions for rotor unbalance response, transient analysis, stability, or for balancing considerations. The gyroscopic moment only causes an increase in the first critical speed of 55 RPM from 2,525 RPM to 2,580 RPM. In the second mode the gyroscopic stiffening causes an increase in the second critical speed of approximately 1,000 RPM.

Figure 2 represents the first three synchronous critical speed mode shapes for the 3-mass Centritech rotor. In order to produce smooth mode shapes without resorting to an excessive number of points, a spline cubic curve fitting procedure has been incorporated into the program to extrapolate additional points along these mode shape curves. Figures 3-5 represent the animated mode shapes for the first three critical speeds for the 3-mass rotor. From the observation of the node points on the animated critical speed mode shapes, it is readily apparent at which positions the non-contacting proximity probes would monitor little rotor motion. For example, if non-contacting probes were mounted close to the bearings, little amplitude could be seen. However, if the probes are mounted at the one quarter span, that is outboard of the #1 and #3 discs, then all three modes may be readily observed.

Figure 6 represents the planar mode for the 3-mass rotor system obtained, using the thermal printer on the HP-9845 computer. In this case, the smoothing procedure was

not used on the mode shapes. Note the distinct difference on the third mode, as shown in Figure 6 and the third mode, as shown in Figure 5 which has smoothing.

Table 2. Synchronous Critical Speed Analysis of Centritech 3-Mass Rotor

Undamped Rotor Mode Shapes and Strain Energy Distribution With Transverse Shear Deformation

NO. 1 CRITICAL SPEED = 2530 ITER= 5 DELTA=-.00011155

ST	X	THETA	M	V	USHAFT	UBEARING
1	-.510	.193	0.0000	0.0000	0	
2	.029	.192	-.0004	-.0001	0	2
3	.232	.190	-.0082	-.0062	0	
4	.633	.135	-.0255	-.0062	8	
5	.670	.135	-.0274	-.0060	0	
6	.774	.135	-.0310	-.0044	0	
7	.815	.131	-.0314	-.0027	1	
8	1.000	-.000	-.0395	-.0025	39	
9	1.000	-.000	-.0402	-.0023	0	
10	1.000	-.000	-.0401	.0001	0	
11	.999	-.005	-.0392	.0025	2	
12	.801	-.135	-.0309	.0026	38	
13	.767	-.135	-.0301	.0028	0	
14	.662	-.135	-.0263	.0046	0	
15	.619	-.139	-.0245	.0061	1	
16	.210	-.191	-.0070	.0062	7	
17	.198	-.191	-.0065	.0062	0	
18	.143	-.191	-.0043	.0062	0	
19	.030	-.191	-.0000	.0063	0	2
20	-.082	-.191	-.0000	.0000	0	
21	-.156	-.191	.0000	.0000	0	

NO. 2 CRITICAL SPEED = 10692 ITER= 6 DELTA= .0001341

ST	X	THETA	M	V	USHAFT	UBEARING
1	.837	-.365	0.0000	0.0000	0	
2	-.178	-.357	.0118	.0033	0	4
3	-.551	-.340	.0618	.0392	0	
4	-.992	.034	.1671	.0374	25	
5	-.983	.035	.1779	.0336	0	
6	-.956	.035	.1741	-.0064	0	
7	-.941	.057	.1602	-.0440	2	
8	-.220	.376	.0124	-.0464	19	
9	-.124	.376	-.0021	-.0472	0	
10	.174	.376	-.0282	-.0524	0	
11	.286	.375	-.0213	-.0454	0	
12	.964	.030	-.1642	-.0447	21	
13	.972	.030	-.1765	-.0409	0	
14	.995	.030	-.1760	-.0014	0	
15	1.000	.007	-.1602	.0377	2	
16	.524	-.334	-.0470	.0400	21	
17	.502	-.335	-.0435	.0411	0	
18	.405	-.336	-.0294	.0416	0	
19	.205	-.339	-.0001	.0424	0	6
20	.005	-.339	.0000	.0002	0	
21	-.125	-.339	.0000	.0002	0	

Table 3

[A] Critical Speed Summary - Synchronous Critical Speed Analysis of Centritech 3-Mass Rotor With Transverse Shear Deformation

NO.	SYNCHRONOUS CRITICAL SPEED ANALYSIS CRITICAL SPEED RPM (HZ)	WMODE LB	ITMODE LB-IN^2	KMODE LB/IN	USHAFT (DIM. STRAIN ENERGY)	UBRG
1	2580 (43)	18.6	7.63E-01	3.52E+03	96	4
2	10692 (178)	17.8	3.05E+00	5.79E+04	90	10
3	26389 (440)	5.2	1.55E+00	1.02E+05	94	6

[B] Critical Speed Summary - Critical Speed Analysis of Centritech 3-Mass Rotor With Transverse Shear Deformation

NO.	PLANAR MODE ANALYSIS CRITICAL SPEED RPM (HZ)	WMODE LB	ITMODE LB-IN^2	KMODE LB/IN	USHAFT (DIM. STRAIN ENERGY)	UBRG
1	2525 (42)	18.5	.8	3355	97	3
2	9697 (162)	18.3	3.7	48839	91	9
3	20771 (346)	14.3	9.3	175081	87	13

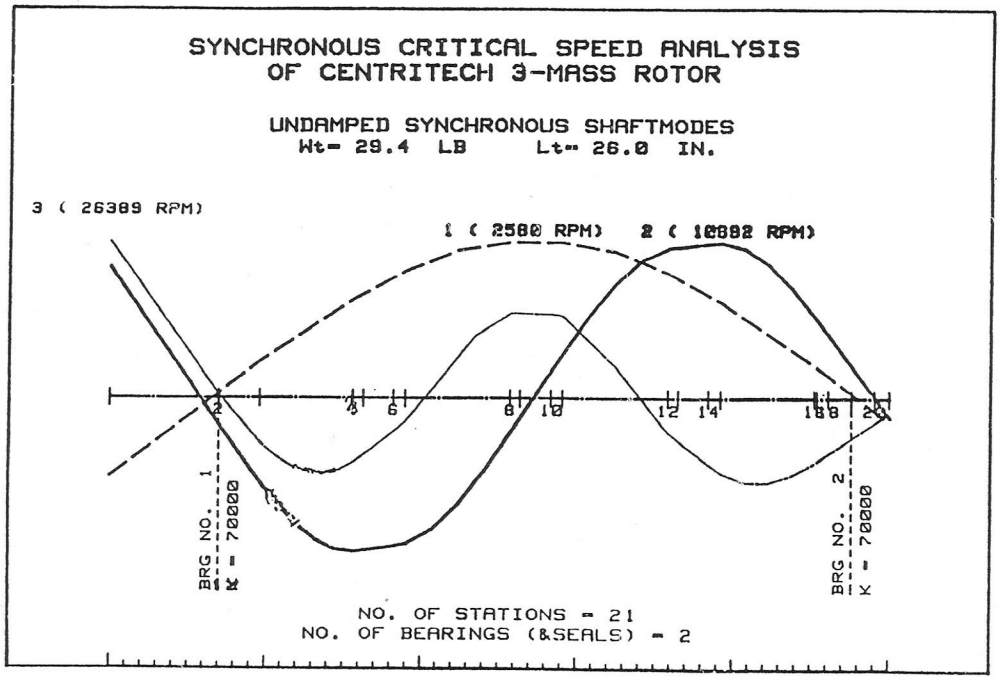

Figure 2. Synchronous Critical Speed Mode Shapes

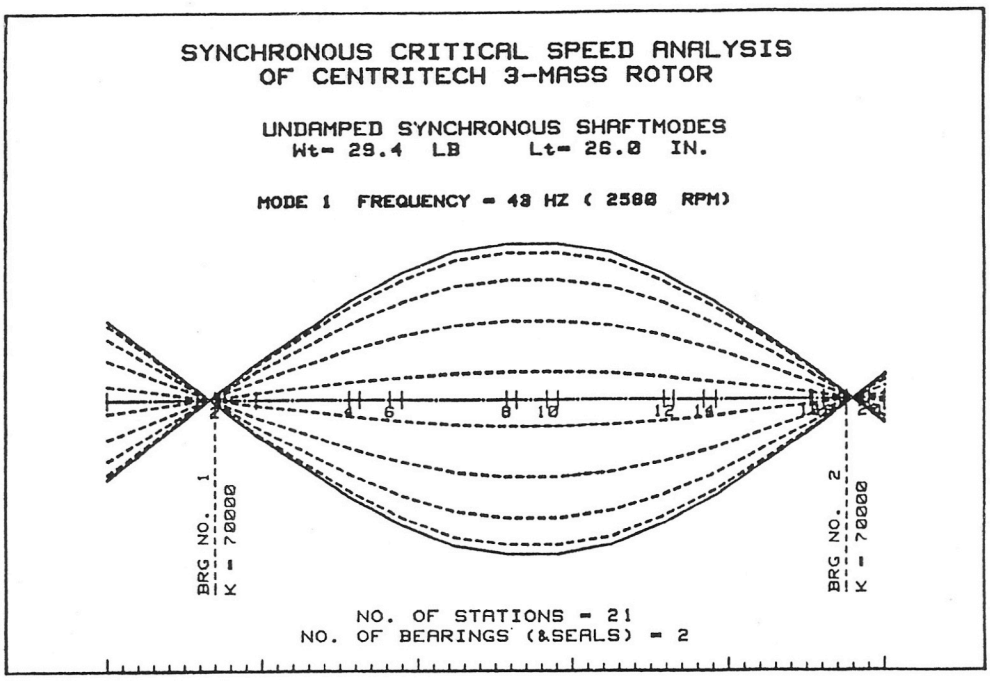

Figure 3. First Critical Speed Mode Shape of Centritech Rotor

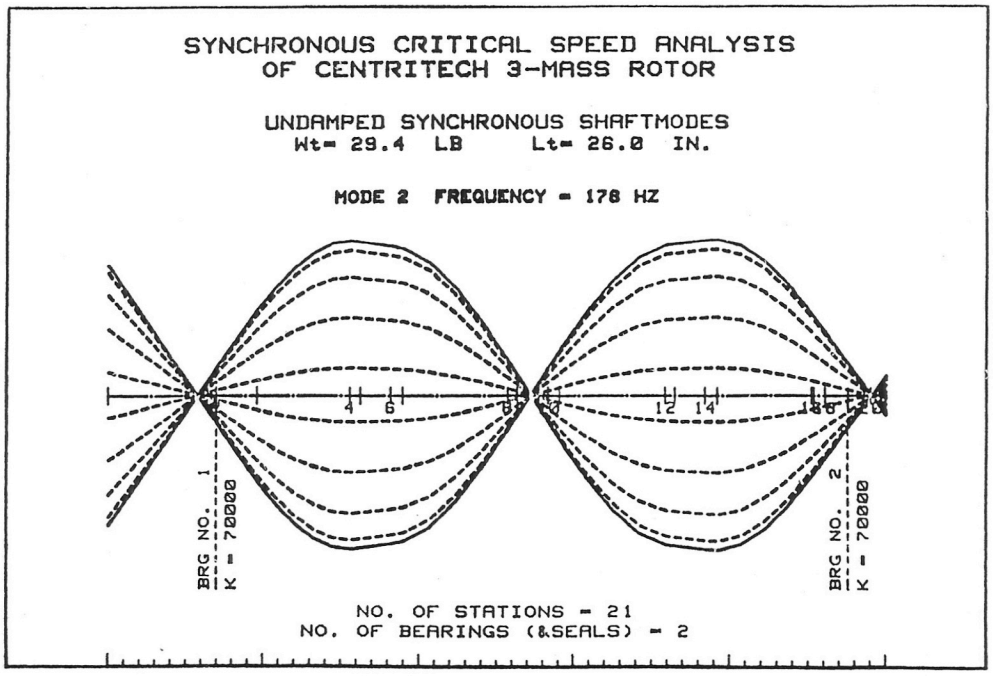

Figure 4. Second Critical Speed Mode Shape of Centritech Rotor

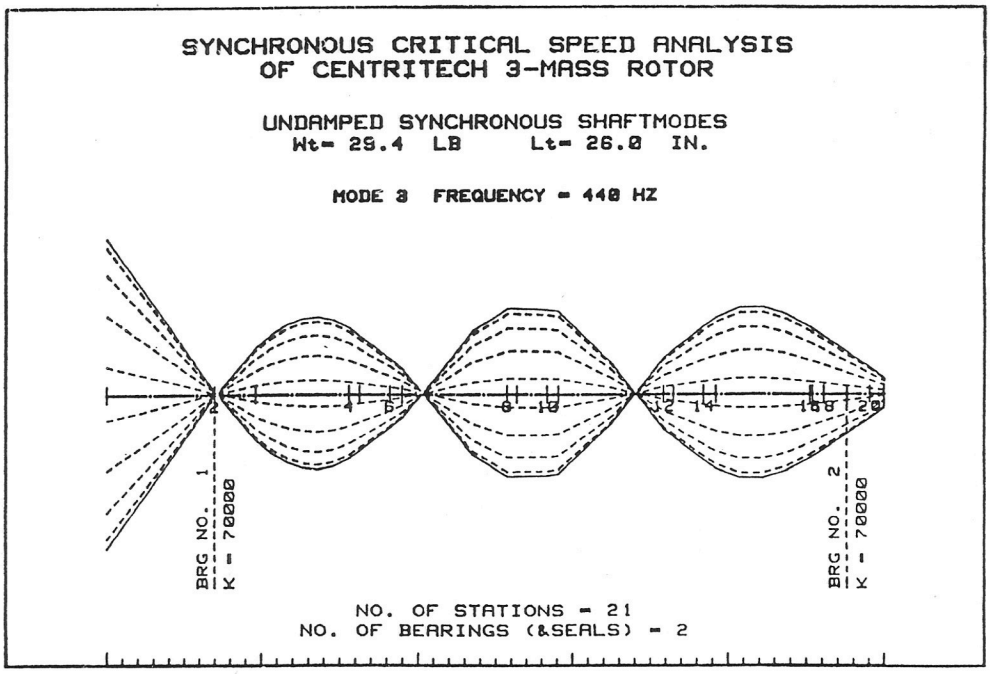

Figure 5. Third Critical Speed Mode Shape of Centritech Rotor

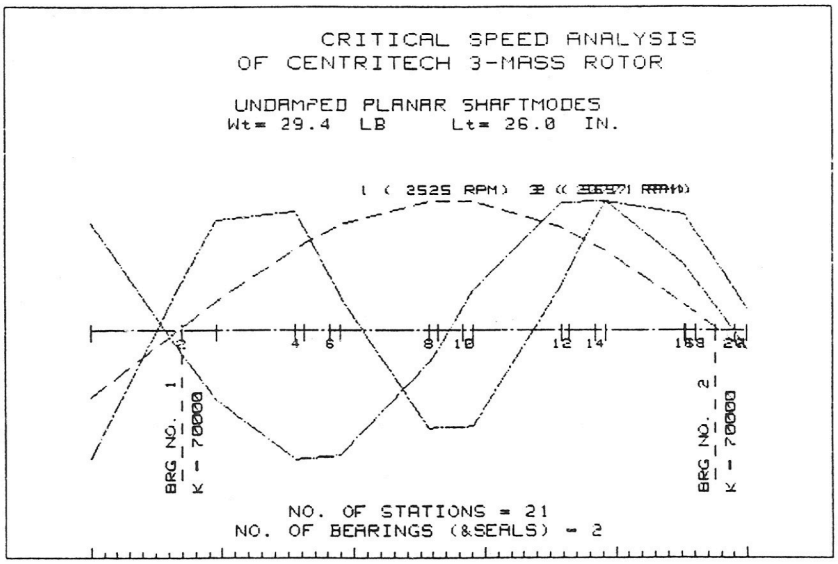

Figure 6. Planar Modes of 3-Mass System
Without Curve Smoothing

HYDRODYNAMIC BEARING COEFFICIENTS AND STABILITY ANALYSIS

The bearings supporting the Centritech rotor are three lobed bearings, L/o = 1.0 with a 50% preload factor. The HP-9845 system was used to generate both the dimensionless as well as the dimensional bearing characteristics at various speeds.

Table 4 represents the dimensionless bearing stiffness and damping coefficients for various values of Sommerfeld number and eccentricity. The Sommerfeld number is expressed in terms of the pad radial clearance C and is given by

$$S = \frac{\mu N_s LD}{W}\left(\frac{R}{C}\right)^2$$

The dimensionless bearing coefficients are given by

$$K_{ij} = \frac{K_{ij}}{(W/C)} \quad ; \quad C_{ij} = \frac{C_{ij}W}{(W/C)}$$

The rigid rotor equations of motion are given by

$$m\ddot{X} + C_{xx}\dot{X} + C_{xy}\dot{Y} + K_{xx}X + K_{xy}Y = F_{x(t)}$$

$$m\ddot{Y} + C_{yy}\dot{Y} + C_{xx}\dot{X} + K_{yx}X + K_{yy}Y = F_{y(t)}$$

The dimensionless stability threshold for the above equations of motion is given by

$$\Omega_s = \omega_s/\omega_g$$

Where $\omega_g = \sqrt{\frac{W}{mc}}$

The dimensionless value of the stability threshold is given in Table 4.

Also shown in Table 4 is the dimensionless whirl speed Nμ. Note that the lowest value of stability occurs at Ec = 0.2 and is given by Ω_s = 3.94. The plain journal

Table 4. Dim Stiffness and Damping Coefficients for a Three Lobe Bearing

L/D = 1.0, Preload Factor = 0.5, LOAD ON PAD

S	Ecc (Dim)	Kxx (Dim)	Kxy	Kyx	Kyy	Cxx	Cxy (Cyx)	Cyy	Nu Whirl RATIO	Ws STAB THRES
3.256	.020	28.31	43.30	-43.40	25.25	94.58	-1.11	88.33	.474	10.91
1.818	.035	16.74	24.39	-24.34	13.70	54.59	-.98	48.27	.474	8.21
1.243	.050	12.21	16.93	-16.72	9.18	38.75	-.84	32.37	.473	6.87
.796	.076	8.82	11.26	-10.82	5.80	26.62	-.61	20.18	.472	5.65
.574	.103	7.24	8.55	-7.90	4.24	20.73	-.37	14.27	.470	4.97
.353	.155	5.91	6.07	-5.02	2.89	15.15	.06	8.70	.464	4.31
.245	.203	5.48	5.01	-3.60	2.36	12.59	.43	6.16	.454	4.04
.181	.246	5.41	4.49	-2.74	2.09	11.20	.73	4.73	.439	3.94
.138	.285	5.54	4.22	-2.12	1.92	10.39	.98	3.81	.415	4.00
.108	.320	5.83	4.10	-1.65	1.80	9.91	1.18	3.16	.379	4.22
.085	.351	6.25	4.08	-1.26	1.71	9.64	1.35	2.67	.325	4.75
.068	.379	6.82	4.13	-.92	1.62	9.54	1.48	2.29	.228	6.55
.062	.389	7.09	4.17	-.79	1.59	9.54	1.52	2.16	.158	9.31
.054	.403	7.56	4.25	-.57	1.54	9.57	1.57	1.92	1.000	999.00
.034	.441	9.70	4.65	.11	1.42	10.03	1.67	1.23	1.000	999.00

bearing only has a dim value of Ω_s of approximately 2.5. Therefore we see that there is a considerable improvement in the stability threshold of a three lobed bearing over a plain journal bearing.

As the Sommerfeld number decreases, the eccentricity increases, and the stability threshold increases. At a Sommerfeld number of .054, the bearing is completely stable.

Table 5 represents the actual bearing stiffness and damping coefficients corresponding to an operating speed of 8500 RPM, and a bearing clearance of C = 2 mils. The bearing clearance is smaller and is given by

$$C_b = C\,[1 - PLF] = 0.5C$$

Where PLF = Preload factor = 0.5

Table 5 shows that for a bearing load of 16 lbs, the vertical bearing stiffness K_{xx} = 73,000 lb/in and the horizontal bearing stiffness K_{yy} = 49,000 lb/in. The critical speed mode shapes were developed for a nominal bearing stiffness value of 70,000 lb/in.

Table 6 represents the bearing synchronous stiffness and damping coefficients as a function of the Sommerfeld number and eccentricity based upon the bearing radial clearance C_b. The synchronous bearing coefficients are determined by assuming that the rotor is moving in a circular orbit. This leads to the approximate bearing coefficients as follows:

$$K_{xxs} = K_{xx} + \omega C_{xy}$$

$$K_{yys} = K_{yy} + \omega C_{xy}$$

$$C_{xxs} = C_{xx} - K_{xy}/\omega$$

$$C_{yys} = C_{yy} + K_{yx}/\omega$$

Table 5. Stiffness and Damping Coefficients for a Three Lobe Bearing

L/D = 1.00 PRELOAD FACTOR = .50

BEARING PARAMETERS;

N = 8500 RPM L = 1.00 IN. D = 1.00 IN. L/D = 1.00
Cbrg = 1.00 MILS Cradial = 2.00 MILS Cb/R = 2.00 MILS/IN
Cbrg = 1.00 MILS Cradial = 2.00 MILS Cb/R = 2.00 MILS/IN
LOAD NUMBER = S*W = 13.28

Sb	W	Eb	Kxx	Kxy	Kyx	Kyy	Cxx	Cxy	Cyy
	(LB)	(DIM)	(LB/IN)*10-3				(LB-S/IN)		
17.024	4.1	.040	57.7	88.3	-88.5	51.5	216.7	-2.5	202.4
7.272	7.3	.070	61.1	89.1	-88.9	50.0	224.0	-4.0	198.1
4.972	10.7	.100	65.2	90.4	-89.3	49.0	232.6	-5.0	194.3
3.184	16.7	.152	73.6	93.9	-90.3	48.4	249.5	-5.7	189.1
2.296	23.1	.206	83.8	98.9	-91.4	49.1	269.5	-4.8	185.5
1.412	37.6	.310	111.2	114.2	-94.4	54.4	320.2	1.3	183.9
.980	54.2	.406	148.5	135.8	-97.6	64.0	383.4	13.1	187.6
.724	73.4	.492	198.5	164.7	-100.5	76.7	461.7	30.1	195.0
.552	96.2	.570	266.6	203.1	-102.0	92.4	561.7	53.0	206.0
.432	123.0	.640	358.5	252.1	-101.5	110.7	684.6	81.5	218.3
.340	156.3	.702	488.3	318.8	-98.4	133.6	846.2	118.5	234.4
.272	195.3	.758	666.0	403.3	-89.8	158.2	1046.7	162.4	251.3
.248	214.2	.778	759.4	446.6	-84.6	170.3	1148.0	182.9	259.9
.216	245.9	.806	929.7	522.6	-70.1	189.4	1322.2	216.9	265.3
.136	390.6	.882	1894.5	908.2	21.5	277.3	2201.0	366.5	269.9

Table 6. Rigid and Flexible Rotor Stability Characteristics and Synchronous Stiffness and Damping Coefficients for a Three Lobe Bearing

L/D = 1.00 PRELOAD FACTOR = .50

BEARING PARAMETERS:

Wt = 26 Lb Wmodal= 19 LB Kmodal= 1021 LB/IN
Ncr= 2750 RIGID SUPPORT CRITICAL SPEED ,RPM
Delta= 19 MILS Shaft Static deflection
N = 8500 RPM OPERATING SPEED ,RPM
L = 1.00 IN. D = 1.00 IN. L/D = 1.00
Cbrg = 1.00 MILS Cradial = 2.00 MILS Cb/R = 2.00 MILS/IN
LOAD NUMBER = S*W = 13.28

Sb	Wb (LB)	Eb	Kxxs (LB/IN)*10-3	Kyys	Cxxs	Cyys	Nsr RIGID ROTOR	Nsf FLEXIBLE STABILITY
13.024	4.1	.040	55.5	49.2	117.5	202.4	59962	3794
7.272	7.3	.070	57.6	46.5	123.9	198.1	60397	5072
4.972	10.7	.100	60.7	44.6	131.0	194.3	61102	6131
3.184	16.7	.152	68.5	43.3	144.0	189.1	62808	7664
2.296	23.1	.206	79.5	44.8	158.3	185.5	65134	9039
1.412	37.6	.310	112.3	55.5	191.9	183.9	71893	11642
.980	54.2	.406	160.2	75.6	230.8	187.6	80892	14253
.724	73.4	.492	225.3	103.5	276.6	195.0	91892	17098
.552	96.2	.570	313.7	139.5	333.6	206.0	106758	20713
.432	123.0	.640	431.0	183.2	401.4	218.3	127287	25577
.340	156.3	.702	593.8	239.1	488.0	234.4	161569	33540
.272	195.3	.758	810.5	302.7	593.6	251.3	249162	53472
.248	214.2	.778	922.2	333.1	646.2	259.9	371084	80660
.216	245.9	.806	1122.8	382.5	735.0	265.3	999999	223500
.136	390.6	.882	2220.7	603.5	1180.6	269.9	999999	249483

Table 6 shows the rigid rotor stability speed in RPM and is given by

$$N_{sr} = \Omega_s \sqrt{\frac{W}{MC}} \times \frac{60}{2\pi}$$

From the critical speed program, one can calculate the critical speed on rigid supports and the corresponding modal mass. The equivalent shaft static deflection δ is given by

$$\omega_{cr} = \sqrt{g/\delta}$$

Hence

$$\delta = g/(N_{cr} \times 2\pi/60)^2$$

Table 6 shows that for a critical speed as low as 2750 RPM, the corresponding δ value is 19 mils.

The value of δ can be used to estimate the stability of the rotor due to shaft flexibility by

$$N_{sf} = \frac{N_{sr}}{\sqrt{1 + K\,(\delta/c)}}$$

Where $K = \dfrac{K_{xx}C_{yy} + K_{yy}C_{xx} - K_{xy}C_{yx} - K_{yx}C_{xy}}{C_{xx} + C_{xy}}$

= dimensionless bearing stiffness parameter.

Therefore it is seen that shaft flex-

bility can have a pronounced effect on reducing the rotor threshold speed. Note that for a 16.7 lb load, with the bearing operating at an eccentricity of 0.152, the rigid rotor stability threshold is over 62,000 RPM. However, when the shaft flexibility is taken into consideration, the stability is greatly diminished to only 7660 RPM. Table 7 represents opening up the bearing clearance from C_b = 1.0 to 2.0 mils. For an 18 lb load on the bearing, note that the stability threshold is around 8400 RPM, which is approximately running speed.

Table 7 also illustrates what would happen if the steady state bearing loading were lost or reduced. If hydraulic loads counteracted the gravitational loading, then the stability threshold would rapidly drop. For a load of only 9.4 lbs, the stability threshold is reduced to 5700 RPM. If on the other hand, the steady state loading can be increased above the gravitational load, then the stability threshold will increase. This is often the case with high speed gear boxes under load. The gear reactions cause sufficiently high loadings to stabilize the rotor. When the gear box

Table 7. Rigid and Flexible Rotor Stability Characteristics and Synchronous Stiffness and Damping Coefficients for a Three Lobe Bearing

L/D = 1.00 PRELOAD FACTOR = .50

BEARING PARAMETERS:

Wt = 26 Lb Wmodal= 19 LB Kmodal= 1021 LB/IN
Ncr= 2750 RIGID SUPPORT CRITICAL SPEED ,RPM
Delta= 19 MILS Shaft Static deflection
N = 8500 RPM OPERATING SPEED ,RPM
L = 1.00 IN. D = 1.00 IN. L/D = 1.00
Cbrg = 2.00 MILS Cradial = 4.00 MILS Cb/R = 4.00 MILS/IN
LOAD NUMBER = S*W = 3.32

Sb	Wb (LB)	Eb	Kxxs (LB/IN)*10-3	Kyys	Cxxs	Cyys	Nsr RIGID ROTOR	Nsf FLEXIBLE STABILITY
13.024	1.0	.040	6.9	6.2	14.7	25.3	21200	1893
7.272	1.8	.070	7.2	5.8	15.5	24.8	21353	2527
4.972	2.7	.100	7.6	5.6	16.4	24.3	21603	3050
3.184	4.2	.152	8.6	5.4	18.0	23.6	22206	3804
2.296	5.8	.206	9.9	5.6	19.8	23.2	23028	4477
1.412	9.4	.310	14.0	6.9	24.0	23.0	25418	5746
.980	13.6	.406	20.0	9.5	28.9	23.4	28600	7019
.724	18.3	.492	28.2	12.9	34.6	24.4	32489	8405
.552	24.1	.570	39.2	17.4	41.7	25.7	37745	10167
.432	30.7	.640	53.9	22.9	50.2	27.3	45003	12538
.340	39.1	.702	74.2	29.9	61.0	29.3	57123	16420
.272	48.8	.758	101.3	37.8	74.2	31.4	88092	26141
.248	53.6	.778	115.3	41.6	80.8	32.5	131198	39410
.216	61.5	.806	140.3	47.8	91.9	33.2	999999	308467
.136	97.7	.882	277.6	75.4	147.6	33.7	999999	342329

is run unloaded, it may be operating in the instability region.

Table 8 represents the stability characteristics with the bearing clearance reduced to 1 mil. This would not be practical because of the heating and excessive horsepower losses. For the case of a rigid rotor, the bearing stability increases as the inverse function of $C^{1/2}$. However, when shaft flexibility is included in the analysis, there is no appreciable gain in stability achieved by drastically reducing the bearing clearance C_b to 0.5 mils. Note that for a bearing load of 16.3 lbs, the stability onset speed is 7600 RPM. It is thus apparent from these stability calculations that this particular 3 lobe bearing is not suitable for use in a compressor design with such a low critical speed and operation to 10,000 RPM is desired. The three lobed bearing has been used extensively in Europe in various turborotors, but it is not satisfactory for this class of machine. In this type of application, it would be preferable to use a tilting pad bearing because of its superior stability characteristics.

Table 8. Rigid and Flexible Rotor Stability Characteristics and Synchronous Stiffness and Damping Coefficients for a Three Lobe Bearing

L/D = 1.00 PRELOAD FACTOR = .50

BEARING PARAMETERS;

Wt = 26 Lb Wmodal= 19 LB Kmodal= 1021 LB/IN
Ncr= 2750 RIGID SUPPORT CRITICAL SPEED ,RPM
Delta= 19 MILS Shaft Static deflection
N = 8500 RPM OPERATING SPEED ,RPM
L = 1.00 IN. D = 1.00 IN. L/D = 1.00
Cbrg = .50 MILS Cradial = 1.00 MILS Cb/R = 1.00 MILS/IN
LOAD NUMBER = S*W = 53.13

Sb	Wb (LB)	Eb	Kxxs (LB/IN)*10-3	Kyys	Cxxs	Cyys	Nsr RIGID ROTOR	Nsf FLEXIBLE STABILITY
13.024	16.3	.040	443.8	393.9	940.0	1619.2	169598	7595
7.272	29.2	.070	460.5	371.7	991.5	1584.8	170827	10161
4.972	42.7	.100	485.9	356.4	1047.8	1554.4	172824	12294
3.184	66.7	.152	547.9	346.4	1151.8	1513.2	177647	15385
2.296	92.6	.206	635.8	358.2	1266.5	1483.9	184226	18167
1.412	150.5	.310	898.5	444.0	1535.3	1471.1	203344	23439
.980	216.8	.406	1281.5	605.0	1846.7	1500.7	228798	28730
.724	293.5	.492	1802.1	827.7	2212.7	1559.8	259909	34495
.552	385.0	.570	2510.0	1116.4	2668.6	1647.9	301956	41821
.432	491.9	.640	3448.2	1465.9	3211.0	1746.4	360023	51678
.340	625.0	.702	4750.0	1912.5	3904.3	1874.9	456987	67814
.272	781.3	.758	6484.4	2421.9	4748.7	2010.1	704737	108198
.248	856.9	.778	7377.5	2664.8	5169.7	2079.4	999999	155547
.216	983.8	.806	8982.1	3059.6	5880.3	2122.2	999999	160050

EXPERIMENTAL ROTOR CHARACTERISTICS

The particular versatility of a minicomputer lies in its ability to collect and process experimental data. The HP-9845 computer was used in conjunction with the Bently ADRE software system and Digital Vector Filter to collect and process both the rotor synchronous and nonsynchronous motion from the Centritech test facility. The use of the HP-9845 computer and the Bently ADRE system has enabled us to obtain data in a fashion that was previously impossible to do. For example, Figure 7 represents the vertical midspan synchronous amplitude and phase and the nonsynchronous motion obtained from the three-mass Centritech rotor supported by multilobe bearings. The rotor was balanced for the first mode. Note that from examination of the experimental data, it is virtually impossible to determine the existence of the first critical speed.

One of the problems with the computer data reduction system is the noise in the signal. This is evidenced by the small irregularity seen in the peak to peak total and synchronous motion plots. Several procedures have been investigated in the Rotor Dynamics Laboratory for numerically smoothing the experimental data in order to remove the noise background. For example, Figure 8 represents the synchronous and nonsynchronous horizontal midspan motion for the same system with curve smoothing. The curve smoothing algorithm was used four times in this procedure.

Since experimental data is saved in a tape file on the computer, it is relatively easy to also subtract the low speed runout. Figure 9 represents the synchronous horizontal midspan motion of the system with curve smoothing and low speed runout subtracted from the synchronous response. Note that there are now three distinct responses apparent in the rotor data. The response at 9800 RPM is the second critical speed. The response at 2500 RPM is the first critical speed.

It is interesting to note that there is a response at approximately 4200 RPM, which corresponds to a resonant condition in the support system. It is now possible, with the curve smoothing procedure, to label the amplitudes and frequencies at which these resonant conditions occur. Note also the substantial difference in the phase angle presentation of Figure 8 and Figure 9.

Another example of the usefulness of the data smoothing procedure is in the polar plot of the Centritech rotor without curve smoothing. Notice that the curve is somewhat irregular. This procedure is even more exaggerated when the RPM increments are not sufficiently close to accurately define the rotor critical speed. When this is the case, one does not obtain a smooth curve in the polar plots, as seen in Figure 10.

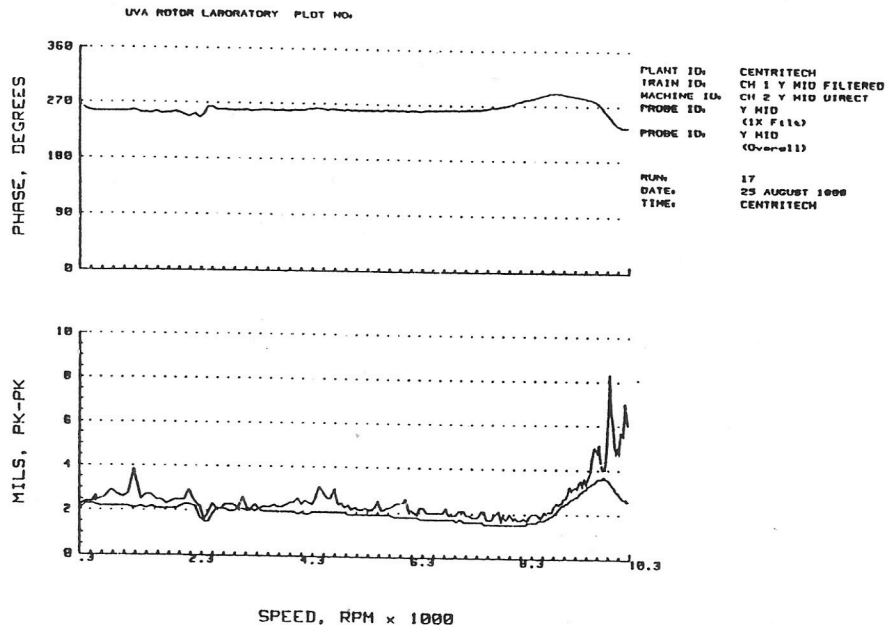

Figure 7. Synchronous and Nonsynchronous Midspan Vertical Motion of the Three-Mass Centritech Rotor -- Balanced First Mode (no smoothing)

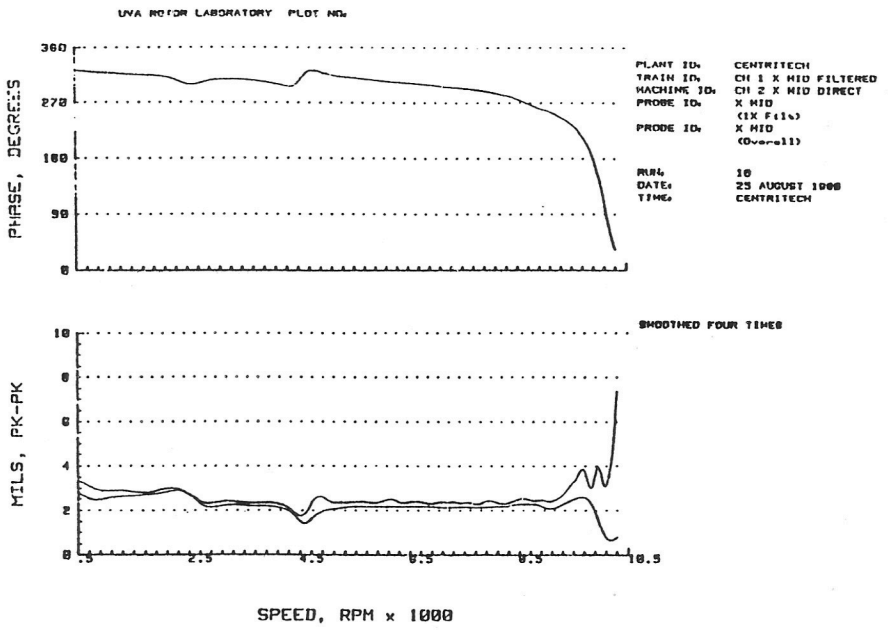

Figure 8. Synchronous and Nonsynchronous Horizontal Midspan Motion of the Three-Mass Centritech Rotor -- Balanced First Mode (numerical smoothing)

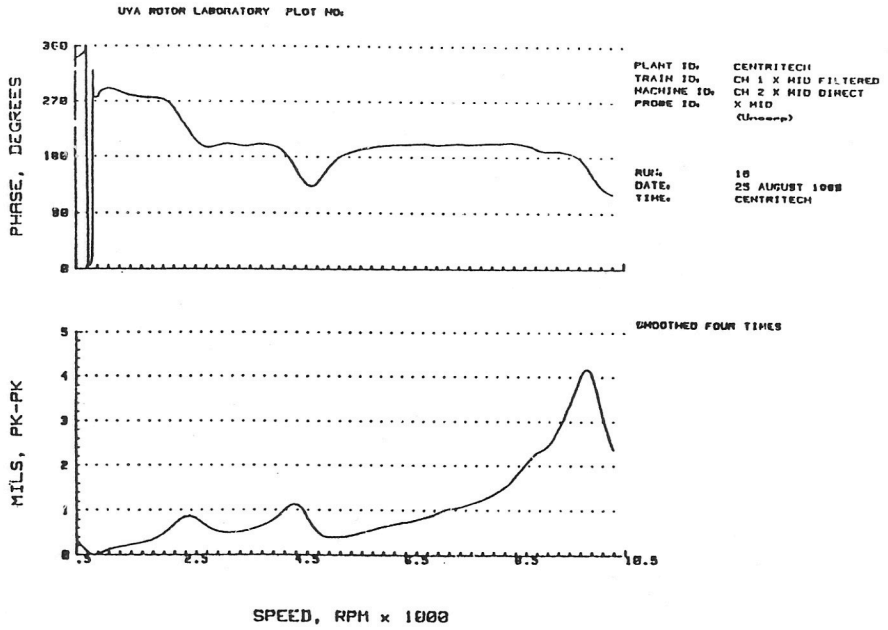

Figure 9. Synchronous Horizontal Midspan Motion of the Three-Mass Centritech Rotor with Curve Smoothing and Run Out Subtraction -- Balanced First Mode

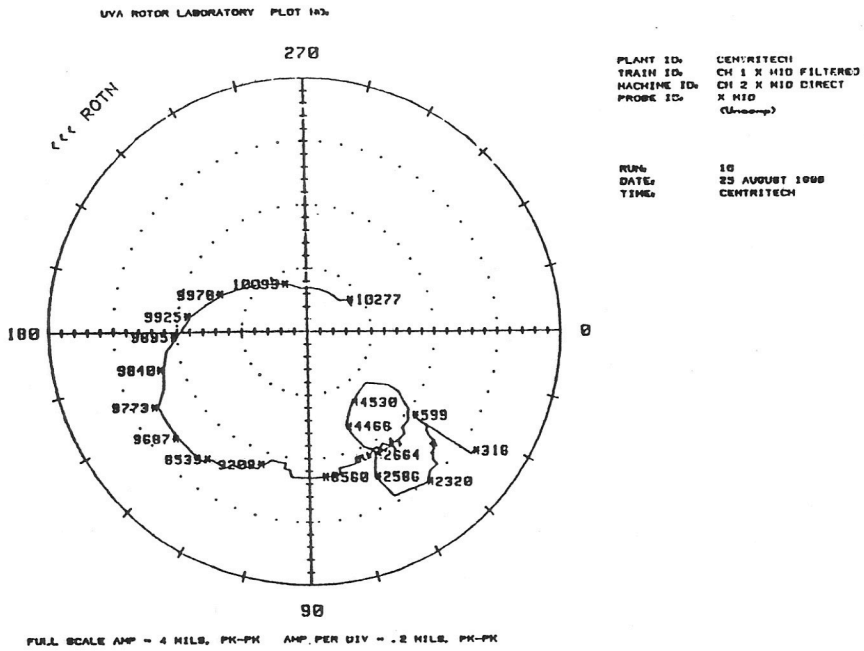

Figure 10. Polar Plot of Horizontal Midspan Motion of the Centritech Rotor Without Curve Smoothing

Figure 11 represents the polar plot with curve smoothing. In addition to the curve smoothing procedure, extrapolation has also been performed to calculate the amplitude and phase at any arbitrary speed. Notice that on this plot the rotor speeds are given corresponding to every 50 RPM.

In the past, polar plots were generated on the Centritech rotor. However, this data has very seldom been used because we were not able to accurately label the corresponding speeds on the polar plot. However, now with the computer system and the ADRE software, plus our extensions to it, we will be able to do some very significant experimental rotor-bearing studies that were impossible to do in the past.

One of the areas of experimental investigation is the determination of rotor modal properties and rotor balancing without trial weights. This material will be discussed in future presentations.

Figure 12 represents the horizontal and vertical midspan motions on the Centritech rotor. The rotor motion shows a considerable amount of low speed runout which is due principally to shaft bow. The rotor first critical speed is excited and the maximum motion is 10 mils in the horizontal directions.

In Figure 13, the rotor was balanced for the first mode by the addition of a correction weight in the center plane. The shaft bow is 2.2 mils peak to peak in the horizontal direction and the shaft unbalance eccentricity e_u is approximately 0.8 mils. A correction weight of 1.62 gm-in was added to the rotor at 90° ahead of the shaft bow vector.

The two runs obtained with and without the addition of the balance weight have been smoothed and stored in the computer file. Intermediate values of amplitude and phase may be interpolated so that the two runs may be subtracted from each other over the entire range of speeds.

Figure 14 represents the net rotor motion at the center plane with the two runs subtracted from each other. This plot represents the dynamic response of the rotor due to a modal unbalance placed upon the rotor. A precise value of the rotor amplification factor may be determined from this rotor by the examination of the rate of change of the phase angle while passing through the critical speed. Also note that the first critical speed of the rotor has been identified to be at 2600 RPM. The dynamic influence coefficient of the rotor at the critical speed is 10.5 mils for 1.62 gm of unbalance at 3 in, or 2.16 mils/gm-in unbalance.

The unbalance moment acting on the rotor is

$$U_t = 1.62 \text{ gm} \times 3 \text{ in radius} = 4.86 \text{ gm-in}$$

The rotor modal weight is

$$W \text{ modal} = 19 \text{ lb}$$

$$e_u = \frac{4.86 \text{ gm-in}}{19 \text{ lb}} \times 2.2 = 0.563$$

A quick estimate of the rotor amplification factor is given by

$$A_c = \frac{X_{max}-(P-P)}{2\ e_u} = \frac{10.}{2 \times 0.563} = \underline{8.88}$$

The rotor therefore is fairly sensitive to unbalance at the first critical speed. This machine would not pass the API specifications for critical speed sensitivity.

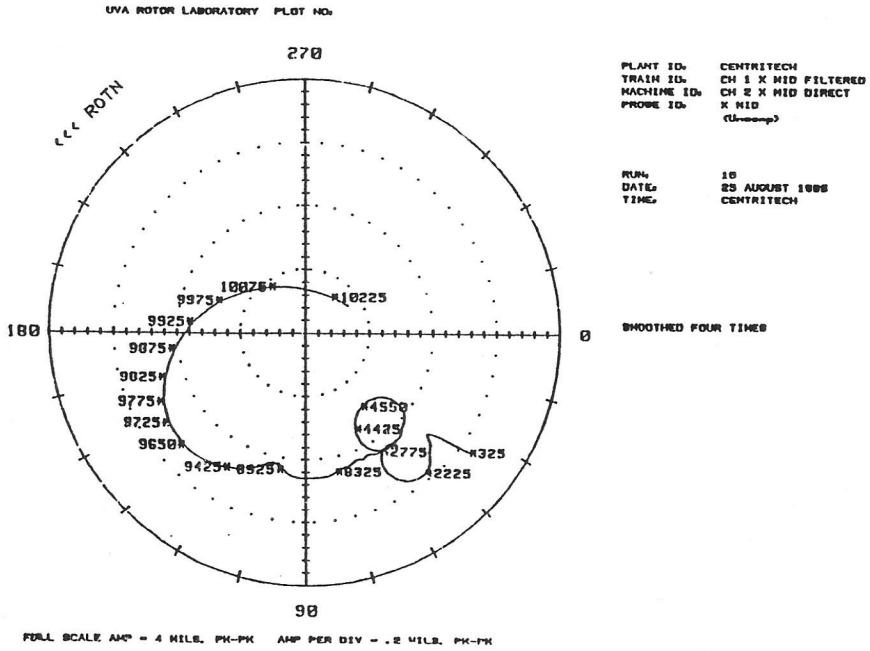

Figure 11. Polar Plot of Horizontal Midspan Motion of the Centritech Rotor With Curve Smoothing

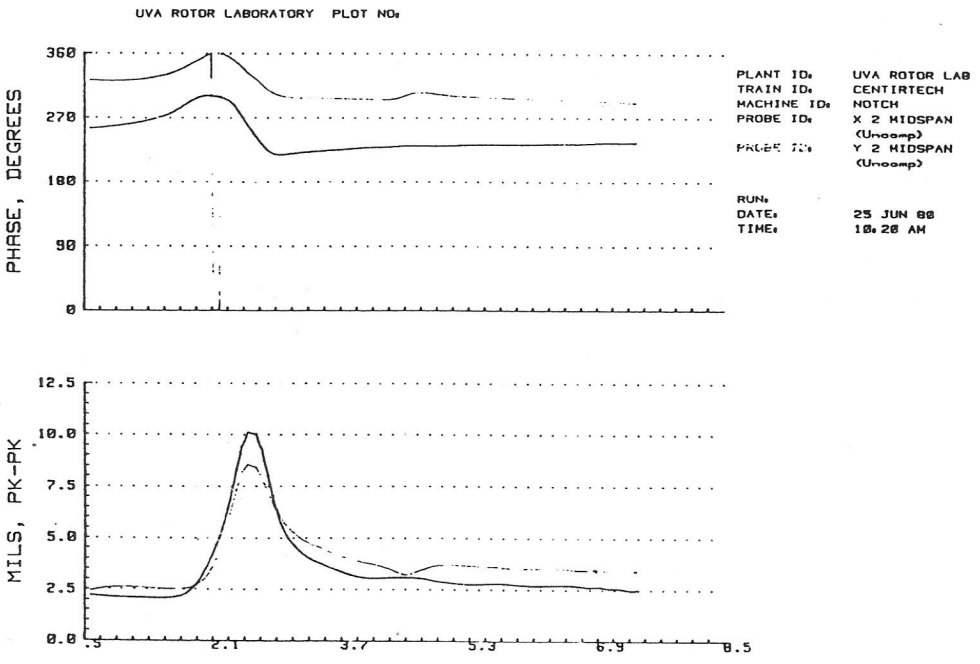

Figure 12

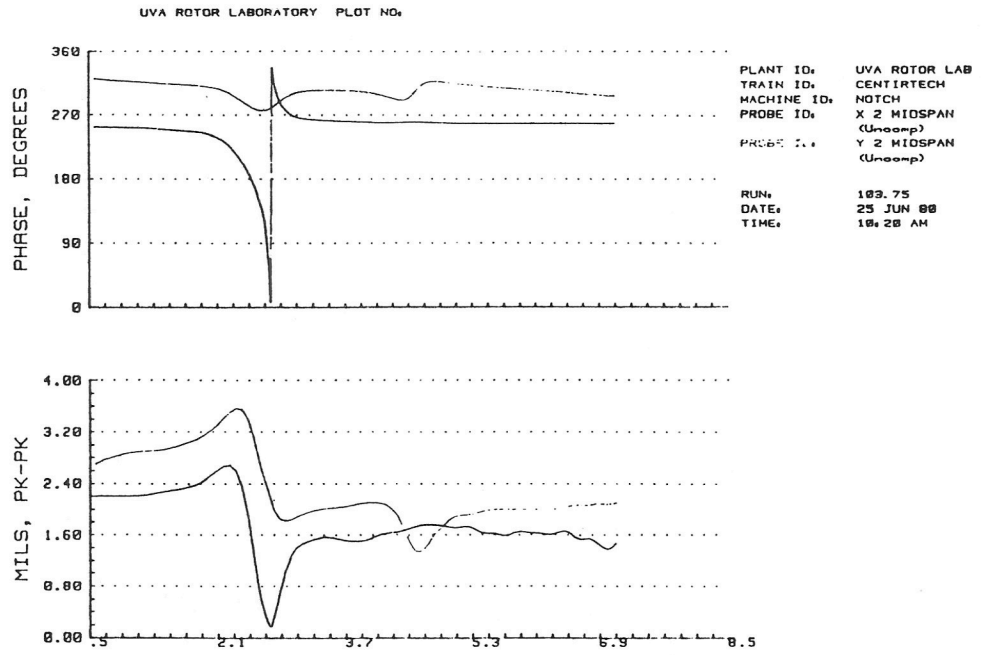

Figure 13

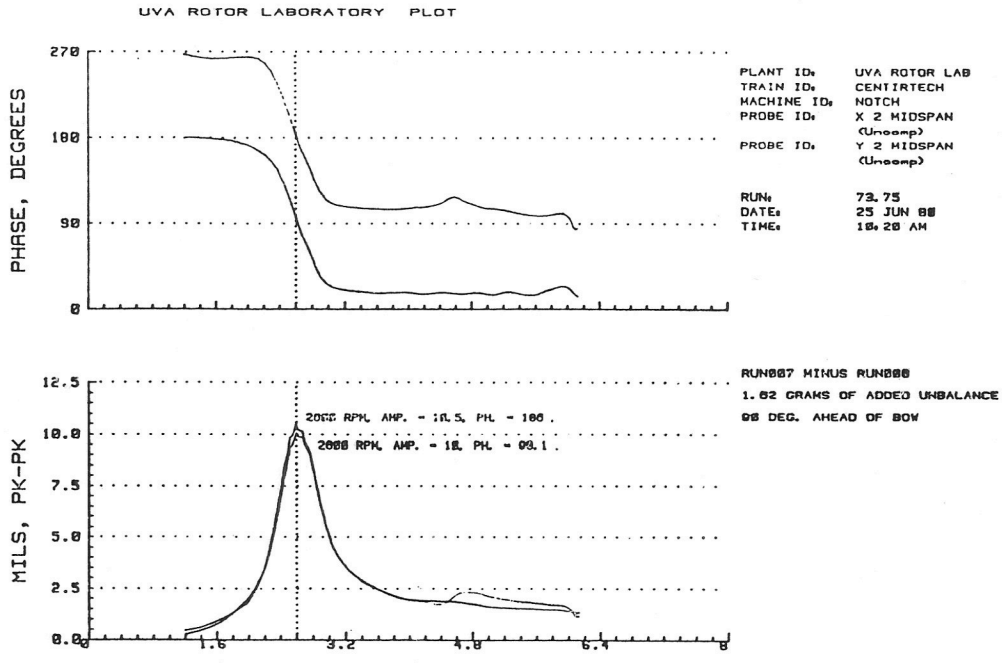

Figure 14

APPENDIX A

CRITICAL SPEED PROGRAM

```
CRITICAL SPEED ANALYSIS BY MATRIX TRANSFER
     METHOD-SINGLE SHAFT ROTOR
 BY E.J.GUNTER UNIV. OF VA. NOV  5,1980

      (SET Ins=1 FOR INSTRUCTIONS)

   LOAD KEY  HELP
        K1=THERMAL PRINTER OUTPUT
        K2=CRT DISPLAY
        K4=DUMP GRAPHICS,THEN PRESS EXECUTE
        K5=DATA

   SET 130 RHO-SHAFT WEIGHT, LB/IN^3
   SET 150 SHEAR=1 FOR TRANSVERSE SHEAR DEFORMATION
                   COWPER EQ. FOR HOLLOW SHAFT
   SET 170 NU,POISSON'S RATIO
   SET 180 E,YOUNG'S MODULUS
   SET 200 EPS - CONVERGENCE CRITERIA

  INPUT DATA FOR CRITICAL SPEED PROGRAM
  -------------------------------------

  READ HEAD1(80) - HEADING                          -940
  READ HEAD2(80) - HEADING                          -950
  READ N,NBR,NCASE,NMODES,MODESHAPE,PLOT            -1010
       N ROTOR STATION DATA LINES
       NBR -NO. OF BEARINGS
       NCASE -NO. OF STIFFNESS CASES-USE 1
       NMODES-NO. OF CRITICAL SPEED MODES-5 MAX
       MODESHAPE-0 NO MODESHAPE CALC
       PLOT -0=NO PLOT,1=CRT PLOT ,2=DIGITAL PLOT
  READ WEXT,L,DEXT,D,DI,IP,IT,TDISC                 -1170
       WEXT=EXTERNAL LUMPED WEIGHT-LB
       L    =SHAFT STATION LENGTH-AFTER MASS STATION
       DEXT=EXTERNAL DISC DIA-FOR CALC OF WDISC&IP
       D    =EXTERNAL SHAFT DIA. FOR INERTIA CALC&WSHAFT
       DI   =INTERNAL SHAFT DIA.
       IP   =DISC POLAR MOMENT OF INERTIA-LB-IN^2
            LUMPED WITH IP CAL. FROM DEXT,D&TDISC
       IT   =DISC TRANSVERSE MONENT OF INERTIA
       TDISC=DISC THICKNESS-CAL. WDISC & IPDISC
  READ LBRG-BEARING STATION NUMBERS,1 TO NBRG -1760
       DO NOT PLACE BRG AT 1ST STATION
  READ K(NBRG)- BEARING STIFFNESS VALUES            -1890
  READ LEFTENDBC ,RIGHTENDBC                        -1920
       FREE ,SIMPLE,FIXED
  READ S / F / B / P1 / O                           -1960
        S    =SYNCHRONOUS CRITICAL SPEEDS
        F    =FORWARD CRITICAL SPEEDS AT SRPM
        B    =BACKWARD CRITICAL SPEEDS AT SRPM
        P1   =PLANAR MODES-NO Ip
        O    =ORDER TRACKING- EX. .5 OR 2
  IF F OR B THEN
  READ SHAFTSPEED, RPM                              -2010
  IF O THEN
  READ ORDER TRACKING RATIO
  READ IRPM,DRPM,FRPM  -SEARCH FREQUENCY RANGE-CPM
```

APPENDIX B

MODAL EXPANSION OF AN ARBITRARY VECTOR

The orthonormal modes dervied from the fundamental equation

$$KX = \lambda MX \tag{1}$$

forms an n dimensional basis in which any arbitrary vector may be expanded. The orthonormal modes themselves have the property that

$$\phi_i^T \; M\phi_j \; = \; \delta_{ij} \tag{2}$$

$$\phi_i^T \; K\phi_i \; = \; \lambda_i \; = \omega_i^2 \tag{3}$$

The orthonormal modes are thus orthogonal with respect to the mass matrix.

Let $\vec{v}$ be an arbitrary vector of dimension n. For example $\vec{v}$ could represent a displacement vector or a forcing function. The vector $\vec{v}$ may be expressed in terms of the orthonormal modes as follows:

$$\{V\} = C_1 \{\phi_1\} + C_2 \{\phi_2\} + C_3 \{\phi_3\} + C_n \{\phi_n\} \tag{4}$$

or

$$\{V\} = \sum_{i=1}^{N} C_i \{\phi_i\} \tag{5}$$

Multiplying by the system mass matrix [m].

$$[m] \{V\} = \sum_{i=1}^{N} C_i [m] \{\phi_i\} \tag{6}$$

The C_i coefficient is determined by multiplying by the j^{th} mode shape

$$\{\phi_j\}^T [M] \{V\} = \Sigma C_i \{\phi_j\}^T [M] \{\phi_i\} \tag{7}$$

Employing the orthogonality condition of Eq 1, we obtain

$$C_i = \{\phi_i\}^T [M] \{V\} \tag{8}$$

A slight variation to Eq (8) is obtained when the mode shapes given are orthogonal displacement modes, but are not in the orthonormal form. In this case, the orthogonality relationship for the displacement modes is given by

$$\{X_i\}^T [M] \{X_j\} = \delta_{ij} M_j \tag{9}$$

Where {X} is an orthogonal displacement mode normalized to unity and M_j is the modal mass, associated with the j^{th} mode.

The expansion of an arbitrary vector in terms of normalized displacement modes is given by

$$\{V\} = \Sigma C_i \{X_i\} \tag{10}$$

Multiplying Eq (10) by $\{X_j\}^T [M]$ yields

$$\{X_j\}^T [m] \{V\} = \sum_{i=1}^{n} \{X_j\}^T [m] C_i \{X_i\} =$$

$$C_i \delta_{ij} M_j \tag{11}$$

Hence, we obtain

$$C_j M_j = \{X_j\}^T [m] \{V\} \tag{12}$$

$$C_j = \frac{\{X_j\}^T [m] \{V\}}{\{X_j\}^T [m] \{X_j\}} \tag{13}$$

Example 1

Given a fourth order system, expand the

arbitrary vector $\{V\}^T = [\ 1\ 0\ 0\ 0\ ]$ in terms of the normalized displacement mode shapes.

The arbitrary vector $\{V\}$ may also be expressed as

$$V_i = X_{ij}\ C_j$$

Where

V_i = i^{th} component of arbitrary vector

X_{ij} = i^{th} displacement component of j^{th} mode.

The complete expansion for the fourth order system would be expressed as

$$\begin{Bmatrix} V_1 \\ V_2 \\ V_3 \\ V_4 \end{Bmatrix} = C_1 \begin{Bmatrix} X_{11} \\ X_{21} \\ X_{31} \\ X_{41} \end{Bmatrix} + C_2 \begin{Bmatrix} X_{12} \\ X_{22} \\ X_{32} \\ X_{42} \end{Bmatrix} + C_3 \begin{Bmatrix} X_{13} \\ X_{23} \\ X_{33} \\ X_{43} \end{Bmatrix} + C_4 \begin{Bmatrix} X_{14} \\ X_{24} \\ X_{34} \\ X_{44} \end{Bmatrix} \quad (14)$$

For example, the component V_1 is given by

$$V_1 = C_1 X_{11} + C_2 X_{12} + C_3 X_{13} + C_4 X_{14} \quad (15)$$

The coefficient C_i may be expressed as

$$C_j = \frac{\{X_j\}^T \{Y\}}{M_j} \quad (16)$$

Where

$$\{Y\} = [m]\ \{V\}$$

In this example, $\{Y\}$ is given by

$$\begin{bmatrix} m_1 & & & \\ & m_2 & & \\ & & m_3 & \\ & & & m_4 \end{bmatrix} \begin{Bmatrix} 1 \\ 0 \\ 0 \\ 0 \end{Bmatrix} = \begin{Bmatrix} m_1 \\ 0 \\ 0 \\ 0 \end{Bmatrix}$$

$$C_j = \frac{[X_{1j}\ X_{2j}\ X_{3j}\ X_{4j}]}{M_j} \begin{Bmatrix} m_1 \\ 0 \\ 0 \\ 0 \end{Bmatrix} = \frac{m_1\ X_{1j}}{M_j}$$

or C_j may also be expressed in terms of the local weight at station i, w_i and the modal weight for the j^{th} mode, w_j, by

$$C_j = \frac{w_1\ X_{1j}}{W_j} \quad (17)$$

Example 2

Based on the results of Example 1, write the coefficients for the following vectors

$$\{V\}_1^T = [\ 1\ 0\ 0\ 0\ ]\quad \{V\}_2^T = [\ 0\ 1\ 0\ 0\ ]$$

$$\{V\}_3^T = [\ 0\ 0\ 1\ 0\ ]\quad \{V\}_4^T = [\ 0\ 0\ 0\ 1\ ]$$

Let the expansions of the above vectors be expressed as

$$\{V\}_1 = \sum_{j=1}^{n} C_{1j}\ \{X\}_j$$

$$\{V\}_i = \sum_{j=1}^{n} C_{ij}\ \{X\}_j$$

From Example 1, the coefficients C_{1j} may be written as

$$C_{1j} = \frac{W_1\ X_{1j}}{W_j} \quad (18)$$

Hence, the general algorithm for the coefficients C_{ij} is

$$C_{ij} = \frac{W_i\ X_{ij}}{W_j}\ ;\ W_j = j^{th} \text{ modal weight} \quad (19)$$

where w_i is the weight at the i^{th} station and j is the j^{th} mode.

The matrix of coefficients (C) represents an influence coefficient for a unitary displacement at the i^{th} location. The coefficients have the property that

$$C_{ij}\ X_{kj} = \delta_{ik} \quad (20)$$

Assume the mass matrix is given by

$$[m] = \frac{1}{g} \begin{bmatrix} 35.56 & & & \\ & 115.58 & & \\ & & 115.58 & \\ & & & 35.56 \end{bmatrix} \quad (21)$$

The modal weights for the n^{th} order system are given by

$$[W]\ \text{modal} = \begin{bmatrix} 241.34 & & & \\ & 133.64 & & \\ & & 74.26 & \\ & & & 152.84 \end{bmatrix} \quad (22)$$

The displacement modes are given by

$$X_1 = \begin{Bmatrix} .378 \\ 1.00 \\ 1.00 \\ .378 \end{Bmatrix};\quad X_2 = \begin{Bmatrix} -1 \\ -.520 \\ .520 \\ 1 \end{Bmatrix}$$

$$X_3 = \begin{Bmatrix} 1 \\ -.116 \\ -.116 \\ 1 \end{Bmatrix};\quad X_4 = \begin{Bmatrix} 1 \\ -.592 \\ .592 \\ -1 \end{Bmatrix} \quad (23)$$

$$C_{11} = \frac{w_1 X_{11}}{W_1} = \frac{35.56 \times .378}{241.34} = .0557$$

$$C_{12} = \frac{w_1 X_{12}}{W_2} = \frac{35.56 \times (-1)}{133.64} = .2661$$

$$C_{13} = \frac{w_1 X_{13}}{W_3} = \frac{35.56 \times 1}{74.26} = 0.4789$$

$$C_{14} = \frac{w_1 X_{14}}{W_4} = \frac{35.56 \times 1}{152.84} = 0.233$$

The expansion of the vector V_1 in terms of the basic set of orthogonal vectors X_i is given by

$$V_1 = .0557\ X_1 - .266\ X_2 + 0.4789\ X_3 + .233\ X_4 \qquad (24)$$

For the vector $V_2^T = [0100]$, the coefficients C_{2j} are given by

$$C_{21} = \frac{w_2 X_{21}}{W_1} = \frac{115.58 \times 1}{241.34} = 0.479$$

$$C_{22} = \frac{-.520 \times 115.58}{113.64} = -0.449$$

$$C_{23} = -.181;\ C_{24} = -0.450$$

The complete C matrix is given by

$$C = \begin{bmatrix} .0557 & -.266 & .479 & .233 \\ .479 & -.449 & -.181 & -.450 \\ .479 & .449 & -.181 & .450 \\ .0552 & .226 & .479 & -.233 \end{bmatrix} \qquad (25)$$

Example 3

Consider the expansion of an arbitrary vector $\{R\}^T = [1111]$ in terms of the C_{ij} coefficients.

$$\text{Let } \{R_1\} = \begin{Bmatrix} R_1 \\ 0 \\ 0 \\ 0 \end{Bmatrix} = R_1 C_{11} \{X_1\} + \text{---} + R_1 C_{14} \{X_4\} \qquad (26)$$

For an arbitrary vector R, the coefficients of the expansion are given by

$$\{R\} = \sum_{j=1}^{N} A_j X_j \qquad (27)$$

Where $A_j = \sum_{i=1}^{n} R_i C_{ij}$

For the vector $\{R\}^T = [1111]$, the coefficients are given by

$$\begin{Bmatrix} 1 \\ 1 \\ 1 \\ 1 \end{Bmatrix} = 1.069\ \{X_1\} + .596\ \{X_3\}$$

Thus, it is seen that the vector $\{R\}$ has components of the 1st and 3rd modes, but not of the 2nd and 4th.

APPENDIX C

STABILITY

CHARACTERISTIC EQUATION

$$M\ddot{u} + C\dot{u} + Ku = F(t) \qquad (1)$$

$$\left[\begin{array}{c|c} M & O \\ \hline O & M \end{array}\right] \begin{Bmatrix} \ddot{u} \\ \dot{u} \end{Bmatrix} + \left[\begin{array}{c|c} C & K \\ \hline -M & O \end{array}\right] \begin{Bmatrix} \dot{u} \\ u \end{Bmatrix} = \begin{Bmatrix} F(t) \\ O \end{Bmatrix} \qquad (2)$$

Let $V = \begin{Bmatrix} \dot{u} \\ u \end{Bmatrix}$

$$\begin{Bmatrix} \ddot{u} \\ \dot{u} \end{Bmatrix} + \left[\begin{array}{c|c} M^{-1}C & M^{-1}K \\ \hline -I & O \end{array}\right] \begin{Bmatrix} \dot{u} \\ u \end{Bmatrix} = \left\{\begin{array}{c} M^{-1}F(t) \\ \hline O \end{array}\right\} \qquad (3)$$

The standard form is given by

$$\{\dot{V}\} - [A]\{V\} = \{R\} \qquad (4)$$

Where

$$A = \left[\begin{array}{c|c} -M^{-1}C & -M^{-1}K \\ \hline I & O \end{array}\right]$$

LEVERRIER'S ALGORITHM

The characteristic polynomial is given by

$$\lambda^n + P_1 \lambda^{n-1} + P_2 \lambda^{n-2} + \ldots P_N = 0 \qquad (1)$$

Where

$$P_1 = -\ \text{Trace}\ [A]$$

$$[B_1] = [A] + P_1 [I]$$

$$P_K = -\frac{1}{K} \text{trace}\ [A\ B_{K-1}] \qquad (2)$$

$$B_K = [A]\ [B_{K-1}] + P_k [I] \qquad (3)$$

Example

Consider a single degree of freedom

system

$$\left[A = \begin{array}{c|c} -C/M & -K/M \\ \hline 1 & 0 \end{array}\right]$$

$$P_1 = -\text{trace } [A] = + C/M$$

$$[B_1] = \left[\begin{array}{c|c} -C/M & -K/M \\ \hline 1 & 0 \end{array}\right] + P_1 \left[\begin{array}{c|c} 1 & 0 \\ \hline 0 & 1 \end{array}\right]$$

$$[B_1] = \left[\begin{array}{c|c} -C/M + C/M & -K/M \\ \hline 1 & C/M \end{array}\right] = \left[\begin{array}{c|c} 0 & -K/M \\ \hline 1 & C/M \end{array}\right]$$

$$[A]\ [B_1] = \left[\begin{array}{c|c} -C/M & -K/M \\ \hline 1 & 0 \end{array}\right] \left[\begin{array}{c|c} 0 & -K/M \\ \hline 1 & C/M \end{array}\right]$$

$$= \left[\begin{array}{c|c} -K/M & 0 \\ \hline 0 & -K/M \end{array}\right]$$

$$P_2 = \frac{-1}{2} \text{ trace } [A]\ [B_1] = \frac{K}{M}$$

Hence, the polynomial is given by

$$\lambda^2 + \frac{C}{M}\lambda + \frac{K}{M} = 0 \qquad (4)$$

$$\lambda = \frac{-\frac{C}{M} \pm \sqrt{\frac{C}{M^2} - \frac{4K}{M}}}{2} = p \pm i\omega d \qquad (5)$$

$$p = -\frac{C}{2m}\left(\frac{\omega_n}{\omega_n}\right) = -\xi\omega_n = \text{real root} \qquad (6)$$

$$\omega_d = \omega_n \sqrt{1 - \xi^2} = \text{damped natural frequency} \qquad (7)$$